

# Superscaling in Lepton-Nucleus Scattering

M. B. Barbaro<sup>1</sup>, J. E. Amaro<sup>2</sup>, J. A. Caballero<sup>3</sup>, and T. W. Donnelly<sup>4</sup>

<sup>1</sup> Dipartimento di Fisica Teorica, University of Turin, and INFN, Sezione di Torino, 10125 Turin, Italy

<sup>2</sup> Departamento de Física Atómica, Molecular y Nuclear, Universidad de Granada, 18071 Granada, Spain

<sup>3</sup> Departamento de Física Atómica, Molecular y Nuclear, Universidad de Sevilla, Apdo. 1065, 41080 Sevilla, Spain

<sup>4</sup> Center for Theoretical Physics, Laboratory for Nuclear Science and Department of Physics, Massachusetts Institute of Technology, Cambridge, MA 02139, USA

**Abstract.** We suggest that superscaling analyses of few-GeV inclusive electron scattering from nuclei, both in the quasielastic peak and in the region where the  $\Delta$ -excitation dominates, allow one to make reliable predictions for charge-changing neutrino reactions at energies of a few GeV, relevant for neutrino oscillation experiments.

## 1 Introduction

Neutrino scattering has been the object of several recent investigations in connection with ongoing and planned experiments exploring neutrino properties, which use nuclei as targets. Moreover, the availability of new neutrino beams and nuclear targets opens the possibility of extracting information on the nucleon's properties, in particular on its strange form factors. For both purposes good control of the nuclear effects is essential for a reliable interpretation of the data.

Present analyses of neutrino oscillation experiments make use of the Relativistic Fermi Gas model, which, although reproducing the gross features of inclusive electron scattering responses, does not account for their detailed structure. As will be shown in the following, relativistic effects play an important role at the kinematical conditions relevant for modern experiments, namely neutrino energies of a few GeV: hence the necessity of more realistic nuclear modeling, which includes relativistic dynamics.

While a number of relativistic calculations for neutrino scattering have been performed recently [1–7], a different approach can also be taken [8, 9]: since any reliable model for neutrino-nucleus cross sections should first be tested against electron scattering experimental data, one can try to extract the neutrino cross sections from the experimental  $(e, e')$  cross sections, where a large amount of data is available.

It has been shown [8, 9] that, in appropriate kinematical conditions, this strategy can be pursued as a consequence of the superscaling properties of the electron scattering data. We shall illustrate this procedure after a brief review of the formalism.

## 2 Electron and Neutrino Scattering: Formalism and Relativistic Fermi Gas

Electron and neutrino scattering off complex nuclei are closely related processes and as such they can be treated within the same formalism.

Apart from obvious differences in the kinematics, due to the leptonic masses involved in the two processes, the basic difference between  $e-A$  and  $\nu-A$  scattering is the nature of the exchanged vector boson, a virtual photon, probing the electromagnetic nuclear current, in the former case and a  $W^\pm$  or a  $Z^0$ , probing the weak current, in the latter.

As a consequence, the corresponding cross sections involve different nuclear response functions and can be in general written in a Rosenbluth-like form as:

$$\left( \frac{d^2\sigma}{d\Omega_e dk'_e} \right)_{(e,e')}^{(EM)} = \sigma_{Mott} [v_L R_L + v_T R_T] \quad (1)$$

$$\left( \frac{d^2\sigma}{d\Omega_l dk'_l} \right)_{(\bar{\nu}, l\mp)}^{(CC)} = \sigma_0^{(CC)} \left[ \widehat{V}_L \widetilde{R}_L + \widehat{V}_T \widetilde{R}_T \pm 2\widehat{V}_{T'} \widetilde{R}_{T'} \right] \quad (2)$$

$$\left( \frac{d^2\sigma}{d\Omega_N dk_N} \right)_{(\bar{\nu}, N)}^{(NC)} = \sigma_0^{(NC)} \left[ v_L \widetilde{R}_L + v_T \widetilde{R}_T + v_{TT} \widetilde{R}_{TT} + v_{TL} \widetilde{R}_{TL} \pm \left( 2v_{T'} \widetilde{R}_{T'} + 2v_{TL'} \widetilde{R}_{TL'} \right) \right] \quad (3)$$

for inclusive electromagnetic (in the extreme relativistic limit  $m_e \rightarrow 0$ ), weak charged-current ( $CC$ , where the outgoing lepton  $l$  is detected) and weak neutral current ( $NC$ , where the nucleon  $N$  is knocked out) reactions, respectively. In the above  $\sigma_{Mott}$  the Mott cross section and  $\sigma_0^{(CC,NC)}$  the analogous quantities for the weak processes,  $v_i$  and  $\widehat{V}_i$  are factors depending upon the lepton kinematics (see [8,9] for their explicit expressions) and the  $\pm$  sign refers to neutrino or antineutrino scattering.

Note that whereas the  $(e, e')$  cross section depends on two electromagnetic response functions,  $R_{L,T}$ , three weak responses,  $\widetilde{R}_{L,T,T'}$ , enter the  $CC$  neutrino scattering due to the presence of the axial weak current. In the  $NC$  reaction three more responses,  $\widetilde{R}_{TT,TL,TL'}$  are involved, similarly to what happens in the semi-inclusive  $(e, e'N)$  process.

Let us first focus on the quasielastic peak, where the dominant process is the knockout of a single nucleon. This domain can be treated in first approximation within the relativistic Fermi gas (RFG) model, where the nucleus is described as a collection of non-interacting Dirac particles. In this case all the response functions in (1,2,3) turn out to be given by

$$(R_i)_{\text{RFG}} = \frac{\mathcal{N}m_N}{qk_F} R_i^{s.n.} f_{\text{RFG}}(\psi), \quad (4)$$

where  $\mathcal{N}$  is the appropriate nucleon number,  $m_N$  the nucleon mass,  $q$  the three-momentum transfer and  $k_F$  the Fermi momentum. Moreover  $R_i^{s.n.}$  are the corresponding single nucleon responses and

$$f_{\text{RFG}}(\psi) = \frac{3}{4}(1 - \psi^2)\theta(1 - \psi^2) \quad (5)$$

is the RFG *superscaling function*, which only depends upon a specific combination of the variable  $q$ ,  $\omega$  (energy transfer) and  $k_F$ , namely the *scaling variable*

$$\psi = \pm \sqrt{\frac{T_0}{T_F}}, \quad T_0 = \left( \frac{q}{2} \sqrt{1 + 1/\tau} - \omega/2 - m_N \right). \quad (6)$$

In Eq. (6)  $T_F$  is the Fermi kinetic energy and  $T_0$  the minimum energy a nucleon in the Fermi sphere must have in order to participate in the reaction at fixed  $q$  and  $\omega$ ,  $\tau = (q^2 - \omega^2)/(4m_N^2)$  being the dimensionless four-momentum transfer. The  $\pm$  sign in (6) refers to values of  $\omega$  smaller ( $-$ ) or larger ( $+$ ) than the quasielastic peak position  $\omega = \sqrt{q^2 + m_N^2} - m_N$ , corresponding to  $\psi = 0$ , and the response region is limited by the  $\theta$ -function in (5) to the range  $-1 \leq \psi \leq 1$ .

We stress that all the response functions, and hence the cross section, can be factorized in a “single-nucleon” function times the superscaling function  $f$ , which only depends upon  $\psi$  and is the same for all nuclei: we then say that the RFG model superscales, namely  $f$  does not explicitly depend upon the momentum transfer  $q$  (scaling of the first kind) nor the Fermi momentum  $k_F$  (scaling of the second kind).

In the  $\Delta$ -resonance peak, centered in  $\omega = \sqrt{q^2 + m_\Delta^2} - m_N$ , all the above expressions still hold providing an appropriate scaling variable

$$\psi_\Delta = \pm \sqrt{\frac{T_0^\Delta}{T_F}}, \quad T_0^\Delta = \left( \frac{q}{2} \sqrt{\rho + 1/\tau} - \omega\rho/2 - m_N \right), \quad (7)$$

accounting for inelasticity through the parameter  $\rho = 1 + (m_\Delta^2 - m_N^2)/(4\tau m_N^2)$ , is used. The RFG model superscales also in the  $\Delta$  region and the associated scaling function is the same as in the quasielastic peak.

### 3 The SuperScaling Analysis (SuSA) of Electron Scattering

An extensive analysis of the world electron scattering data based on the superscaling ideas introduced above has been performed in the quasielastic domain [10] by studying a reduced cross section, obtained as the ratio of the experimental ( $e, e'$ ) cross section and the appropriate single-nucleon factors, as a function of the scaling variable (6).

The analysis has shown that for high enough energies scaling of the first kind is fulfilled at the left of the quasielastic peak (the so-called scaling region) and broken at its right, whereas scaling of the second kind is very well satisfied at the left of the peak and not so badly violated at its right. Moreover, the scaling violations have

been found to reside mainly in the transverse channel, whereas in the longitudinal scaling is very good.

As a result a phenomenological superscaling function  $f(\psi)$  has been constructed which fits the electron scattering longitudinal response for all the available momentum transfers and nuclear species. The deviations from the total (longitudinal and transverse) data can be ascribed to two contributions: 1) the excitation of the  $\Delta$ -resonance and 2)  $q$ - and  $k_F$ -dependent nuclear effects such as meson exchange currents and their associated correlations, which break both kinds of scaling. Although the exact calculation of these effects is very involved [11–14], their net effect in the quasielastic region can be assessed to be roughly 10–15%.

The superscaling function, plotted in Figure 1 versus  $\psi'$  (the “prime” indicates an energy shift, of about 20 MeV, necessary to reproduce the right experimental position of the quasielastic peak), significantly differs from the RFG one due to nuclear interactions not included in the Fermi gas model. In particular, it is lower, it extends over a wider range of  $\psi'$  and, importantly, it displays an asymmetric shape, with a pronounced tail in the  $\psi' > 0$  region. This peculiar feature of the superscaling function, which has been further investigated in recent work [2, 5, 15], represents a stringent constraint on any reliable microscopic model.

The same analysis has been recently extended to the  $\Delta$  peak [8] by first subtracting the quasielastic cross section calculated by means of the phenomenological superscaling function from the total experimental data and then analyzing the result in terms of the scaling variable  $\psi_\Delta$  defined in Eq. (7). This procedure removes from the data the impulsive (i.e., elastic eN) contributions that arise from quasielastic scattering. The corresponding reduced cross section (namely, divided by the appro-

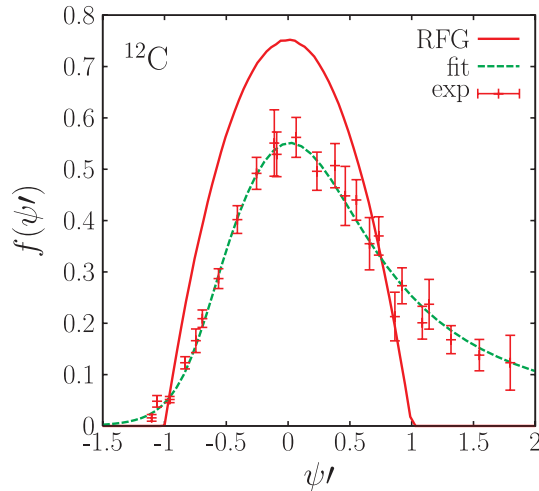


Figure 1. The experimental quasielastic superscaling function together with its phenomenological fit (dashed green) and the RFG result (solid red) plotted versus the corresponding scaling variable  $\psi'$ .

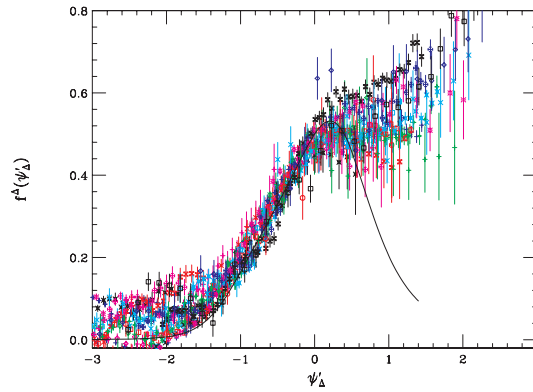


Figure 2. The experimental  $\Delta$  superscaling function for the world data on carbon and oxygen and its phenomenological fit (solid line) plotted versus the corresponding scaling variable  $\psi'_\Delta$ .

appropriate elementary  $N \rightarrow \Delta$  function) has been shown to superscale reasonably well for negative values of  $\psi_\Delta$ , indicating that the dominant process contributing to the cross section in this region has been correctly identified as the  $N \rightarrow \Delta$  excitation. For positive values of  $\psi_\Delta$  this is no longer the dominant process since other resonances and the tail of deep inelastic scattering come into play.

As a result a phenomenological superscaling function  $f^\Delta(\psi_\Delta)$ , fitting the subtracted data, has been constructed in analogy with what was done in the quasielastic case (see Figure 2).

A test of the two phenomenological superscaling functions is presented in Figure 3, where the data are compared with the result obtained by inserting these functions into the RFG responses (4) in place of  $f_{\text{RFG}}$ . In [8] the same test is performed at different kinematical conditions and for different nuclei, showing that the superscaling approach yields a very satisfactory representation of the electron scattering data for a wide range of kinematics, for energy transfer lower than the one corresponding to the  $\Delta$  peak.

#### 4 Application of SuSA to Neutrino and Antineutrino Scattering

Having succeeded in representing the inclusive electron scattering data by means of two “universal” (namely,  $q$ - and  $A$ -independent) superscaling functions, valid in the quasielastic and  $\Delta$ -dominance regions respectively, we can now reverse the procedure and give predictions for neutrino and antineutrino reactions.

Let us first focus on the charged-current process. Since the kinematics of  $(e, e')$  and  $(\nu, \mu)$  are strictly related, the procedure simply amounts to multiplying the phenomenological scaling function by the appropriate elementary neutrino-nucleon factor in order to construct the differential cross section (2).

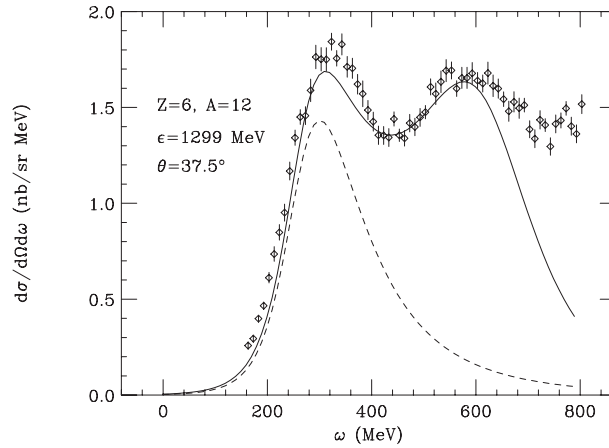


Figure 3. The experimental  $(e, e')$  cross section for  $^{12}\text{C}$  compared with the SuSA prediction including both the quasielastic and  $\Delta$  contribution (solid curve). The dashed curve represents the pure quasielastic cross section.

The assumption underlying this procedure is that the superscaling function associated to the three responses in (2) is the same and is equal to the one associated to the electromagnetic responses in (1). While this is guaranteed by CVC as far as the vector-isovector components of the responses are concerned (i.e. the ones arising from the vector nuclear current), for the axial components it is not exactly true, since the axial current is only partially conserved. However, at the intermediate-to-high energies we are considering here, both the axial and vector operators reduce, in the non-relativistic limit, to  $\sigma^{-1}$ : hence the corresponding scaling functions should be the same. This argument neglects higher order contributions like meson exchange currents, which of course act differently in the different channels, and go in any case beyond the present analysis.

In Figure 4 we show the double differential quasielastic CC neutrino cross section with respect to the outgoing muon momentum  $k'$  and solid angle  $\Omega$  as a function of  $k'$ , for neutrino energy of 1 GeV and muon scattering angle of 90 degrees.

It appears that the superscaling analysis prediction (solid red) is significantly lower and wider than the RFG result (dashed green), reflecting the differences observed in Figure 1. For comparison the non-relativistic Fermi gas result (dotted violet) is also shown in order to stress the importance of relativistic effects in this energy domain. Indeed these not only move the peak position and produce a shrinking of the response region due to the relativistic kinematics, but they also yield a change in size due to the correct Dirac “spinology”. It clearly appears from Figure 4 that relativistic effects cannot be neglected. Whereas they can be accounted for exactly in the simple Fermi gas model, some efficient prescriptions which can be used

<sup>1</sup> Although we deal with relativistic effects exactly, this argument can be made more clearly in the non-relativistic limit.

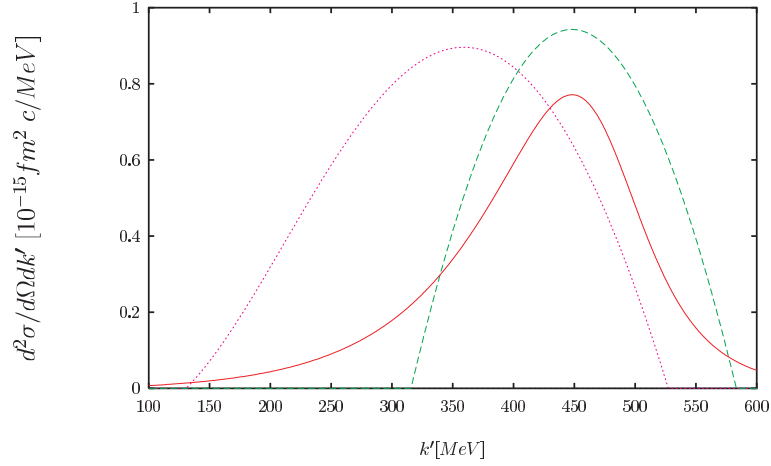


Figure 4. Double differential ( $\nu_\mu, \mu^-$ ) cross section versus the outgoing muon momentum  $k'$  for neutrino energy  $E_\nu = 1$  GeV and muon scattering angle  $\theta_\mu = 90^\circ$ . Dashed (green): relativistic Fermi gas; dotted (violet): non-relativistic Fermi gas; solid (red): SuSA result.

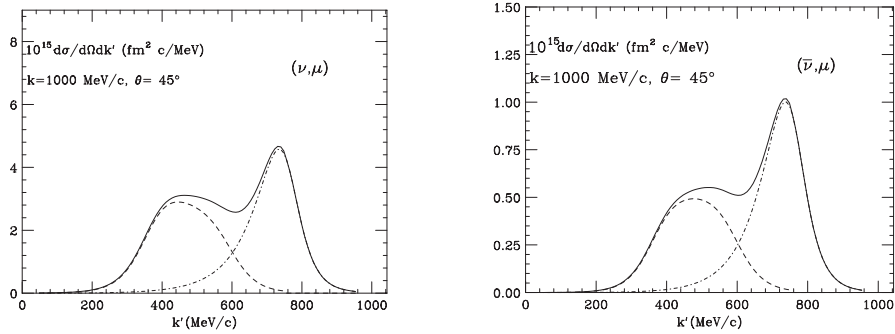


Figure 5. The SuSA cross section for the charged-current reactions ( $\nu_\mu, \mu^-$ ) (left panel) and ( $\bar{\nu}_\mu, \mu^+$ ) (right panel) on  $^{12}\text{C}$  plotted versus the final-state muon momentum  $k'$ . The dash-dotted curves give the QE contribution, the dashed curves the  $\Delta$  contribution and the solid curves the total.

in order to “relativize” more sophisticated nuclear calculations have been recently developed and successfully tested on the relativistic shell model [1].

In Figure 5 the neutrino and antineutrino differential cross sections are shown for  $E_\nu = 1$  GeV and scattering angle of 45 degrees, including also the  $\Delta$  contribution (left peak). Note that the antineutrino cross section is about 5 times smaller than the neutrino one, the difference becoming more dramatic as the scattering angle increases (see [8]). The reason is that the contributions of the responses  $\tilde{R}_T$  and  $R'_T$  to the cross section are almost equal in size, but they add for neutrino and interfere destructively for antineutrino scattering. As a consequence small changes in the

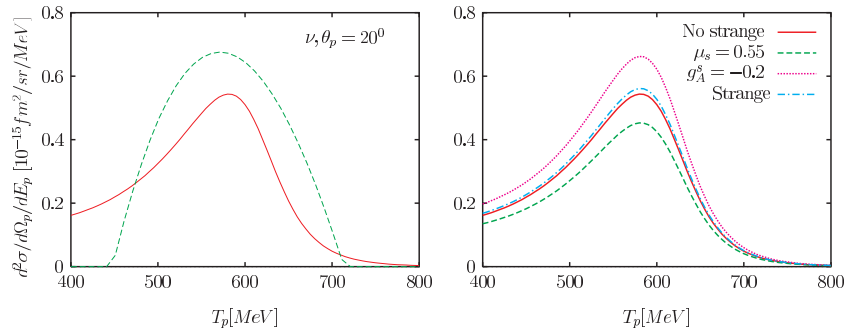


Figure 6. Double differential neutral current neutrino cross section for proton knockout with respect to the proton energy and solid angle plotted versus the proton kinetic energy. The neutrino energy is 1 GeV and the proton scattering angle 20 degrees. Left panel: the SuSA prediction (solid red) is compared to the RFG result (dashed green). Right panel: effects of variations of the magnetic (dashed green), axial (dotted violet) or both magnetic and axial (dotdashed cyan) strange form factors of the proton, compared with the result without strangeness (solid red).

model, as the inclusion of two-body currents, could have very large effects on the  $\bar{\nu}$  result, which should therefore be taken with great caution.

In the case of neutral current reactions, the kinematics are different from the one of CC processes and of  $(e, e')$ . In fact, while the CC reaction is a  $t$ -scattering type process (the Mandelstam variable  $t$  is fixed), the NC is a  $u$ -scattering process, since the detected final state is the outgoing nucleon, and the neutrino kinematic variables are integrated over [16]. This in turn implies an integration region in the residual nucleus variables which is different in the two cases. As a consequence, it is not obvious that the superscaling procedure, based on the analogy with inclusive electron scattering, is still valid.

This issue is discussed at length in [9], where it is shown that the scaling method is based on a factorization assumption which has been tested numerically, with the outcome that the procedure can be applied also to neutral current reactions.

In Figure 6 (left panel) we show the results for quasielastic neutrino scattering and proton knockout calculated in both the RFG model (dashed green) and the SuSA approach (solid red). More results, corresponding to antineutrino scattering and to neutron knockout, are given in [9].

As for the CC case, it appears that the results based on superscaling are significantly different from the ones of the non-interacting model and the almost parabolic RFG cross section is strongly deformed by the nuclear dynamics implicit in the phenomenological scaling function.

Finally, in Figure 6 (right panel) we show results obtained by allowing for a non-zero strange quark content of the nucleon: we compare our predictions for the cross section in a situation where no strangeness is assumed (solid red) with the ones obtained including strangeness in the magnetic (dashed green) and axial-vector (dotted violet) form factors, using for  $\mu_s = G_M^{(s)}(0)$  a representative value extracted

from the recent world studies of parity-violating electron scattering and taking  $g_A^s = G_A^{(s)}(0)$  to be  $-0.2$  [17]. The effects from inclusion of electric strangeness are not shown here, since  $G_E^{(s)}$  has almost no influence on the full cross sections.

These results, which show a strong sensitivity of the cross section to the strangeness content of the nucleon, are in line with the well-known fact (see, e.g., [16, 18]) that the NC reactions can be used, together with parity-violating electron scattering [19, 20], to measure the strange form factors of the nucleon.

## 5 Conclusions

We have shown how the large amount of existing ( $e, e'$ ) data can be used to predict neutrino-nucleus cross sections, of interest for the search of neutrino oscillations and for the measurements of the nucleon strange form factors.

The method we have developed is based on the superscaling properties displayed by the electron scattering data both in the quasielastic peak and in the  $\Delta$ -excitation region.

Beyond the practical usefulness of the SuSA procedure, this study opens several interesting questions connected to the microscopical description of the superscaling function and in particular to its strongly asymmetric shape, which represents a powerful test of different nuclear models.

We believe that, for energies not too low, the superscaling analysis yields predictions for neutrino scattering at the 15–20% level, the uncertainty being related to the violations of superscaling. These mainly arise from two body contributions (meson-exchange currents and their associated correlations) which are not included in our phenomenological representation of the nuclear dynamics.

## References

1. J. E. Amaro, M. B. Barbaro, J. A. Caballero, T. W. Donnelly and C. Maieron, *Phys. Rev. C* **71**, 065501 (2005).
2. J. A. Caballero, J. E. Amaro, M. B. Barbaro, T. W. Donnelly, C. Maieron and J. M. Udias, *Phys. Rev. Lett.* **95**, 252502 (2005).
3. A. N. Antonov *et al.*, *Phys. Rev. C* **74**, 054603 (2006); nucl-th/0609056.
4. A. Meucci, C. Giusti and F. D. Pacati, *Nucl. Phys. A* **739**, 277 (2004).
5. J. A. Caballero, *Phys. Rev. C* **74**, 015502 (2006).
6. A. Botrugno and G. Co', *Nucl. Phys. A* **761**, 200 (2005).
7. O. Benhar, N. Farina, H. Nakamura, M. Sakuda and R. Seki, *Phys. Rev. D* **72**, 053005 (2005).
8. J. E. Amaro, M. B. Barbaro, J. A. Caballero, T. W. Donnelly, A. Molinari and I. Sick, *Phys. Rev. C* **71**, 015501 (2005).
9. J. E. Amaro, M. B. Barbaro, J. A. Caballero and T. W. Donnelly, *Phys. Rev. C* **73**, 035503 (2006).
10. T. W. Donnelly and I. Sick, *Phys. Rev. C* **60**, 065502 (1999); *Phys. Rev. Lett.* **82**, 3212 (1999); C. Maieron, T. W. Donnelly and I. Sick, *Phys. Rev. C* **65**, 025502 (2002).

11. J. E. Amaro, M. B. Barbaro, J. A. Caballero, T. W. Donnelly and A. Molinari, *Nucl. Phys. A* **643**, 349 (1998).
12. J. E. Amaro, M. B. Barbaro, J. A. Caballero, T. W. Donnelly and A. Molinari, *Nucl. Phys. A* **723**, 181 (2003).
13. J. E. Amaro, M. B. Barbaro, J. A. Caballero, T. W. Donnelly and A. Molinari, *Phys. Rept.* **368**, 317 (2002).
14. A. De Pace, M. Nardi, W. M. Alberico, T. W. Donnelly and A. Molinari, *Nucl. Phys. A* **741**, 249 (2004).
15. A. N. Antonov *et al.*, *Phys. Rev. C* **71**, 014317 (2005).
16. M. B. Barbaro, A. De Pace, T. W. Donnelly, A. Molinari and M. J. Musolf, *Phys. Rev. C* **54**, 1954 (1996).
17. K. A. Aniol *et al.* [HAPPEX Collaboration], *Phys. Lett. B* **635**, 275 (2006); K. A. Aniol *et al.* [HAPPEX Collaboration], *Phys. Rev. Lett.* **96**, 022003 (2006); D. S. Armstrong *et al.* [G0 Collaboration], *Phys. Rev. Lett.* **95**, 092001 (2005).
18. W. M. Alberico *et al.*, *Nucl. Phys. A* **623**, 471 (1997).
19. M. J. Musolf, T. W. Donnelly, J. Dubach, S. J. .. Pollock, S. Kowalski and E. J. Beise, *Phys. Rept.* **239**, 1 (1994).
20. T. W. Donnelly, M. J. Musolf, W. M. Alberico, M. B. Barbaro, A. De Pace and A. Molinari, *Nucl. Phys. A* **541**, 525 (1992).